Optical solitary waves escaping a wide trapping potential in nematic liquid crystals

Citation for published version:
Assanto, G, Minzoni, AA, Peccianti, M & Smyth, NF 2009, 'Optical solitary waves escaping a wide trapping potential in nematic liquid crystals: Modulation theory', *Physical Review A*, vol. 79, no. 3, 033837. https://doi.org/10.1103/PhysRevA.79.033837

Digital Object Identifier (DOI):
10.1103/PhysRevA.79.033837

Link:
Link to publication record in Edinburgh Research Explorer

Document Version:
Publisher's PDF, also known as Version of record

Published In:
Physical Review A

Optical solitary waves escaping a wide trapping potential in nematic liquid crystals: Modulation theory

Gaetano Assanto,[1,*] Antonmaria A. Minzoni,[2,†] Marco Peccianti,[3,‡] and Noel F. Smyth[4,§]

[1]*Department of Electronic Engineering, Nonlinear Optics and OptoElectronics Lab (NooEL), INFN-CNISM-University of Rome "Roma Tre," Via della Vasca Navale 84, 00146 Rome, Italy*

[2]*Department of Mathematics and Mechanics, Fenomenos Nonlineales y Mecánica (FENOMEC), Instituto de Investigación en Matemáticas Aplicádas y Sistemas, Universidad Nacional Autónoma de México, 01000 México D.F., México*

[3]*Research Center SOFT INFM-CNR, University "Sapienza," P. A. Moro 2, 00185 Rome, Italy and UOP-Group, INRS-EMT, Université du Québec, Varennes, Quebec, Canada J3X 1S2*

[4]*School of Mathematics and Maxwell Institute for Mathematical Sciences, The King's Buildings, University of Edinburgh, Edinburgh EH9 3JZ, Scotland, United Kingdom*

(Received 22 December 2008; published 24 March 2009)

A nonlinear extension of geometric optics is used to derive a modulation theory solution for the trajectory of an optical solitary wave in a nematic liquid crystal—i.e., a *nematicon*—in which a wide waveguide has been defined by an externally applied static electric field. This solution is used to find the power threshold for the solitary wave to escape the trapping waveguide. This threshold is found to be in excellent agreement with experimental results.

DOI: 10.1103/PhysRevA.79.033837 PACS number(s): 42.65.Tg, 42.70.Df

I. INTRODUCTION

The trapping of linear waves by gradients in the refractive index of the medium in which they propagate is a classical one [1]. In addition, the scattering of solitary waves by single [2–4] as well as multiple dielectric interfaces [5] has received substantial theoretical attention; experimental results in self-focusing glasses with a thermal nonlinearity have also been reported [6,7]. Experimental demonstrations with optical spatial solitons in nematic liquid crystals, so-called nematicons [8], have been carried out at single linear and nonlinear interfaces [9], as well as voltage [10–12] or all-optically induced interfaces [13]. In recent work, Peccianti *et al.* [14] experimentally studied the bouncing of $2D+1$ nematicons in wide voltage-induced waveguides or potential traps and how the effectiveness of the trapping varied with the soliton power, with the self-localized beams being able to escape the waveguide or potential barrier when they had sufficient power or effective kinetic energy.

In the present work modulation theory concepts are used [15,16] to provide a nonlinear counterpart of the classical linear waveguide analysis based on geometric optics [1], and provide a theoretical framework for and comparison with experimental results [14]. With a simplified approximation for the static electric field which defines the waveguide via electro-optic reorientation, momentum conservation for a nematicon is employed in deriving a nonlinear equivalent to the geometric optics ray path. The equation for the nematicon trajectory is then used to find the threshold power for the solitary wave to escape the waveguide formed by the externally applied static electric field. This threshold is found to be in excellent agreement with experimental data [14], a remarkable result given the approximations adopted to cast the theoretical solution.

II. ESCAPE CRITERION

In dimensional form, the equations governing the propagation of a light beam through a nematic liquid crystalline cell with planar anchoring, as employed in Ref. [14] (see Fig. 1), are

$$2ik_0n_0\frac{\partial E}{\partial Z}+\nabla^2E+k_0^2[n^2(Y)+n_\perp^2\cos^2\psi+n_\parallel^2\sin^2\psi-n_\perp^2\cos^2\psi_0-n_\parallel^2\sin\psi_0]E=0, \tag{1}$$

$$K\nabla^2\psi+\frac{\Delta\epsilon_{\rm RF}}{2}E_s^2\sin 2\psi+\frac{\epsilon_0n_a^2}{4}|E|^2\sin 2\psi=0. \tag{2}$$

Here $n_a^2=n_\parallel^2-n_\perp^2$ relates to the optical anisotropy (the subscripts refer to the optic axis of the equivalent uniaxial), K is the elastic constant of the nematic liquid crystal (NLC) in the single constant approximation (i.e., the same for splay, bend, and twist of the molecules [17,18]), ϵ_0 is the permittivity of free space, and $\Delta\epsilon_{\rm RF}$ the low-frequency anisotropy, with $\Delta\epsilon_{\rm RF}\approx 9\epsilon_0$ for E7, a commercially available NLC. The field E_s is the static (or low-frequency) electric field used to define the waveguide encoded in the index of refraction $n(Y)$ via reorientation [14]. Let us set $\psi=\psi_0+\theta$, where ψ_0 does not depend on Y, and assume that θ is small. Nematicon Eqs. (1) and (2) can then be set in normalized form using the nondimensional variables $E=Au$, $Z=Bz$, $X=Wx$, and $Y=Wy$, where

$$B=\frac{4n_0}{k_0n_a^2\sin 2\psi_0},\quad W=\frac{2}{k_0n_a\sqrt{\sin 2\psi_0}}. \tag{3}$$

A typical optical power P_t is related to A and B by $P_t=\pi A^2W^2/2$ for a Gaussian beam, the latter being a standard

*assanto@uniroma3.it
†tim@mym.iimas.unam.mx
‡m.peccianti@gmail.com
§N.Smyth@ed.ac.uk

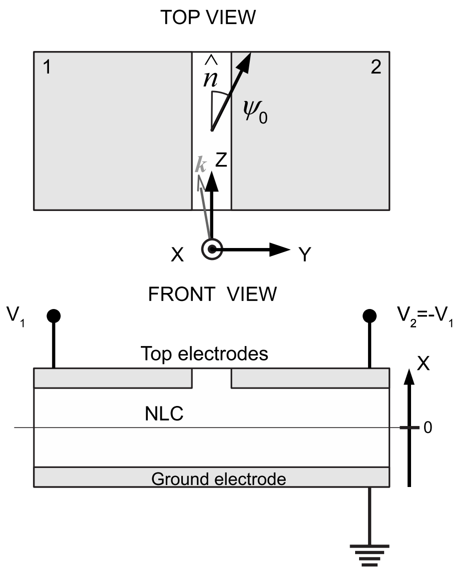

FIG. 1. Sketch of the geometry and cell layout. The nematic liquid crystal is confined in a sandwichlike structure with the molecular director lying in the cell plane YZ at an angle θ_0 with Z. Two top electrodes [(1) and (2)] and a bottom ground electrode enable the application of a quasistatic field. The top electrodes are biased by π phase-shifted voltages V_1 and V_2, resulting in a significant Y component of the electric field under the interelectrode gap, i.e., a confining potential owing to reorientation. A nematicon is generated by launching a Gaussian beam with wave vector $\mathbf{k}$ at an angle with Z.

approximation for the nematicon transverse profile [19]. Based on the small deviation assumption ($|\theta|$ small), nematicon Eqs. (1) and (2) become

$$iu_z + \frac{1}{2}\nabla^2 u + 2\theta u + m(y)u = 0, \tag{4}$$

$$\nu\nabla^2\theta - 2q(y)\theta + 2|u|^2 = 0, \tag{5}$$

where

$$\nu = \frac{8K}{\epsilon_0 n_a^2 A^2 W^2 \sin 2\psi_0},$$

$$q(y) = \frac{4\Delta\epsilon_{\rm RF}}{\epsilon_0 n_a^2 A^2 \tan 2\psi_0} E_s^2(y), \tag{6}$$

$$m(y) = \frac{2n^2(y)}{n_0^2 n_a^2 \sin 2\psi_0}. \tag{7}$$

To determine the criterion for the escape of a nematicon from the waveguide, we shall use conservation of momentum for Foch-Leontovich Eq. (4). It should be noted that the term conservation of momentum is here meant in terms of invariances of the Lagrangian for nematicon Eqs. (4) and (5) rather than physically conserved quantities for light [20]. It can be shown that this momentum conservation equation is

$$i\frac{d}{dz}\int_{-\infty}^{\infty}\int_{-\infty}^{\infty}(u^* u_y - uu_y^*)dxdy = \int_{-\infty}^{\infty}\int_{-\infty}^{\infty}(-2|u|^2 m_y + 2\theta^2 q_y)dxdy. \tag{8}$$

The integrals in the relation above can be evaluated once the nematicon is identified (so that u and θ are known), and the variations in the refractive index $n(y)$ and static electric field $E_s(y)$, and hence $q(y)$, across the waveguide are known. Unfortunately, there is no exact nematicon solution in 2+1 dimensions. However, a good approximation to it has been found using trial functions in an averaged Lagrangian formulation of nematicon Eqs. (4) and (5) [15]. Minzoni *et al.* [15] used both sech and Gaussian trial functions for the nematicon. For ease in calculating the integrals in momentum Eq. (8), here we shall use the Gaussian trial functions

$$u = a\exp\{-[x^2 + (y-\xi)^2]/w^2\}e^{i\sigma z + iV(y-\xi)}, \tag{9}$$

$$\theta_n = \alpha\exp\{-[x^2 + (y-\xi)^2]/\beta^2\}, \tag{10}$$

where θ_n is the change in director angle (i.e., optic axis) due to the self-localized beam. The relations between the optical amplitudes and widths a and w, and the director amplitudes and widths α and β are given in Minzoni *et al.* [15] but they will not be needed here. What will be needed is the ratio

$$\frac{\alpha^2\beta^2}{a^2w^2} = \frac{8P^{4/5}}{\pi^{4/5}\nu^{7/5}q^{2/5}}, \tag{11}$$

where P is the optical power

$$P = \int_{-\infty}^{\infty}\int_{-\infty}^{\infty}|u|^2 dxdy = \frac{\pi}{2}a^2w^2. \tag{12}$$

As the nematicon evolves in the potential, its amplitude and width oscillate. If the diffractive radiation shed by the nematicon as it evolves is neglected, then optical power (12) is conserved, and the oscillations of the amplitude and width decouple from the position evolution [21].

The experimental results of Peccianti *et al.* [14] (Figs. 2 and 3) show that E_s within the waveguide can be approximated by a parabolic profile. In nondimensional form we then have

$$\frac{E_s^2(y)}{A^2} = \gamma_2(L^2 - y^2), \tag{13}$$

for $-L \le y \le L$. The physical half-width $\tilde{L}$ of the waveguide is related to the nondimensional width by $\tilde{L} = WL$. If the value of E_s at the center of the waveguide is E_{sc}, then $\gamma_2 = E_{sc}^2/(A^2L^2)$.

To complete the determination of the nematicon trajectory, we need the refractive index distribution in the waveguide. From standard birefringence in uniaxial crystals, we have

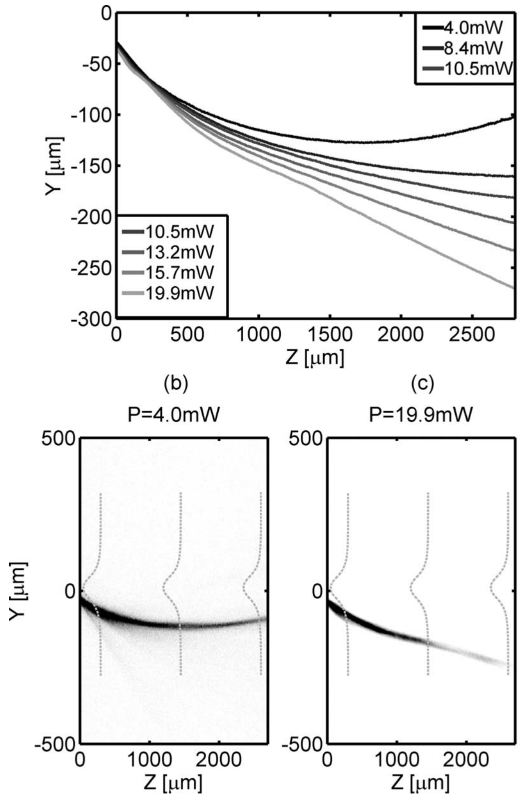

FIG. 2. Sample data from experiments on optical solitons ($\lambda = 1064$ nm) escaping a bias-induced graded-index potential. (a) Mean soliton path for various input excitations: at low power the solitons are trapped in the potential, whereas for $P > 15$ mW their initial momentum permits them to escape and propagate straight in the surrounding nonlinear dielectric. [(b) and (c)] Photographs showing the propagation of a nematicon in the voltage-defined guiding profile for an optical input power of (b) 4 and (c) 19.9 mW, respectively. The latter case is that of an escaping soliton.

$$n = \frac{n_\perp n_\parallel}{\sqrt{n_\parallel^2 \cos^2 \psi + n_\perp^2 \sin^2 \psi}}. \tag{14}$$

The change in director orientation θ in the waveguide has two components: θ_1 due to the voltage-defined potential well or waveguide through the NLC electro-optic response and θ_n, given by Eq. (10), caused by the nematicon through nonlinear reorientation. To first order the refractive index in the waveguide can be calculated from θ_1, which is then used to calculate the contribution due to $m(y)$ in momentum Eq. (8). Setting $\psi = \psi_0 + \theta_1$ and expanding for small θ_1 gives

$$n = n_1(1 + n_2\theta_1), \tag{15}$$

where

$$n_1 = \frac{n_\perp n_\parallel}{\sqrt{n_\parallel^2 \cos^2 \psi_0 + n_\perp^2 \sin^2 \psi_0}},$$

$$n_2 = \frac{(n_\parallel^2 - n_\perp^2)\sin 2\psi_0}{2(n_\parallel^2 \cos^2 \psi_0 + n_\perp^2 \sin^2 \psi_0)}. \tag{16}$$

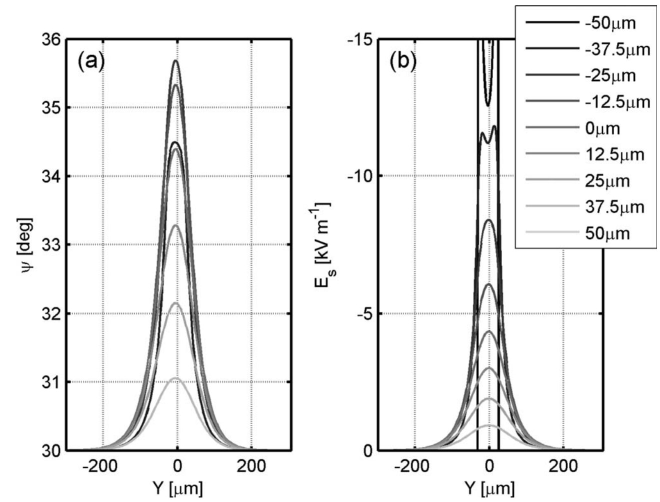

FIG. 3. Numerical integration of the NLC governing equations. (a) The Y distribution of the in-plane reorientation angle ψ and (b) the Y component of the static field E_s, respectively, are graphed at different altitudes X across the thickness of the cell, from $X = -50$ μm to $X = 50$ μm The vertical dashed lines indicate the edges of the two top electrodes for the applied bias.

The change in orientation angle within the waveguide due to the field $E_s(y)$ can be obtained by solving director Eq. (5) with $u = 0$. This leads to a solution for θ_1 in terms of parabolic cylinder functions, which results in the integral involving $m(y)$ in momentum Eq. (8) being impossible to evaluate analytically. However, as for the electric field E_s in the waveguide, the results of Peccianti *et al.* [14] show that the change in orientation angle in the potential trap due to $E_s(y)$ can again be approximated by a quadratic form so that

$$\theta_1 = \frac{\theta_c}{L^2}(L^2 - y^2), \tag{17}$$

where θ_c is the value of θ_1 in the waveguide midplane $y = 0$. Figure 3 shows the numerically calculated field E_s due to the electrodes and the applied voltage. It can be seen that the field is nearly parabolic except for spikes near the electrode edges. This point will be discussed further below.

Substituting the expressions for $q(y)$, with E_s given by Eq. (13), and $m(y)$, with $n(y)$ given by Eq. (15), into the momentum conservation Eq. (8), we obtain the equation

$$\frac{dV}{dz} = \frac{d^2\xi}{dz^2} = \left[2q_c\gamma_2 \frac{\alpha^2\beta^2}{a^2w^2} - \frac{8n_2\theta_c}{n_a^2 L^2 \sin 2\psi_0} \right]\xi \tag{18}$$

for the position of the nematicon in the waveguide. It should be stressed that the nematicon contribution $\theta^2 q_y$ was calculated with $\theta = \theta_n$, given by Eq. (10). Here

$$q_c = \frac{4\Delta\epsilon_{\mathrm{RF}}}{\epsilon_0 n_a^2 A^2 \tan 2\psi_0}. \tag{19}$$

It is noted that the next order contribution to $n(y)$ from θ_n could be added to Eq. (18) but this contribution is not needed as this momentum equation gives results in excellent agreement with experiments. On setting $\xi' = V = V_0$ as the launch-

TABLE I. Parameter values used here and pertinent to the experiments of Ref. [14].

Parameter	Dimensional value
λ_0	1064 nm
$n_\parallel$	1.6954
$n_\perp$	1.5038
K	1.2×10^{-12} N
$\Delta\epsilon_{\mathrm{RF}}$	$9\epsilon_0$
ψ_0	30°
ψ at center of waveguide	36°
$\tilde{L}$	200 μm
V_0	0.16
ξ_0	30 μm
E_{sc} at center of waveguide	1.25×10^4 V/m
P_t used for nondimensionalization	10.2 mW

ing angle of the input beam at $\xi=\xi_0$ and integrating once, we have

$$\left(\frac{d\xi}{dz}\right)^2 = V_0^2+\left[2q_c\gamma_2\frac{\alpha^2\beta^2}{a^2w^2}-\frac{8n_2\theta_c}{n_a^2L^2\sin 2\psi_0}\right](\xi^2-\xi_0^2). \tag{20}$$

The critical power for the beam to be just trapped in the waveguide is then given by the condition that the turning point of the nematicon trajectory $\xi'=0$ occurs at $\xi=L$. So from Eq. (20) the nematicon trajectory has a turning point at

$$\xi_t^2=\frac{V_0^2+\dfrac{8n_2\theta_c}{n_a^2L^2\sin 2\psi_0}\xi_0^2-2q_c\gamma_2\dfrac{\alpha^2\beta^2}{a^2w^2}\xi_0^2}{\dfrac{8n_2\theta_c}{n_a^2L^2\sin 2\psi_0}-2q_c\gamma_2\dfrac{\alpha^2\beta^2}{a^2w^2}}. \tag{21}$$

The soliton then escapes the waveguide if $\xi_t>L$. Using the parameter values in Table I, the critical power for escape from the trap is $P_c=18.7$ mW for a waveguide of effective width of 200 μm. This is in excellent agreement with the experimental estimate of 16–18 mW [14], especially given the number of approximations made in the theoretical analysis. The dependence of the turning point ξ_t of the nematicon trajectory on the input power is shown in Fig. 4. The parabolic approximation for the electric field E_s is accurate around the center of the waveguide, where the electric field is around 1.25×10^4 V/m. It is less accurate in the tails where the electric field has a more Gaussian decay. In particular, the parabolic approximation gives a sharp field cutoff rather than the smooth decay seen in Fig. 3. However, such a sharp cutoff is smoothed out in the averaging process used to derive the momentum Eq. (8), which explains the accurate results obtained.

Integrated momentum Eq. (20) can also be used to predict the exit angle of the nematicon when it escapes the waveguide. This angle is given by $d\xi/dz$ at $\xi=L$. The measured output angles of the nematicon are given in Fig. 5, noting that these values were evaluated irrespective of whether the

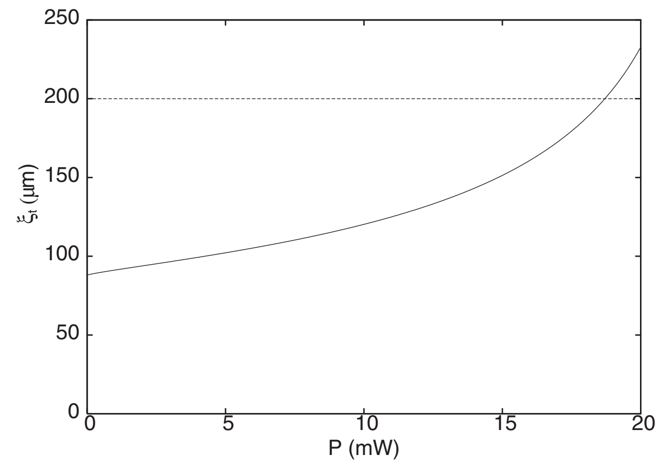

FIG. 4. Turning point of nematicon trajectory as given by Eq. (21) with the parameter values given in Table I.

nematicon escaped the waveguide. In agreement with turning point expression (21), in this figure the nematicon escapes the waveguide for $P=19.9$ mW, as also displayed in the photograph, Fig. 2(c). Even though the experimental escape angle is slightly smaller than the theoretical prediction of 79.5 mrad from Eq. (20), the latter results from a one-dimensional scalar calculation and does not account for birefringent walk off. Finally, the noninclusion of (Rayleigh) scattering in the model, although the related propagation losses are visible in Fig. 2(c), does not appear to affect the validity of the theory and its good agreement with the experimental results.

III. DISCUSSION AND CONCLUSIONS

The analysis leading to the nematicon trajectory of Eq. (20) explains in simple terms the nonlinear mechanism whereby a nematicon can escape a waveguide. At low power the initial kinetic energy of the beam is not large enough to overcome the potential barrier defined by the imposed refractive index distribution. While the launch angle of the input beam was kept constant in the experiments of Peccianti *et al.*

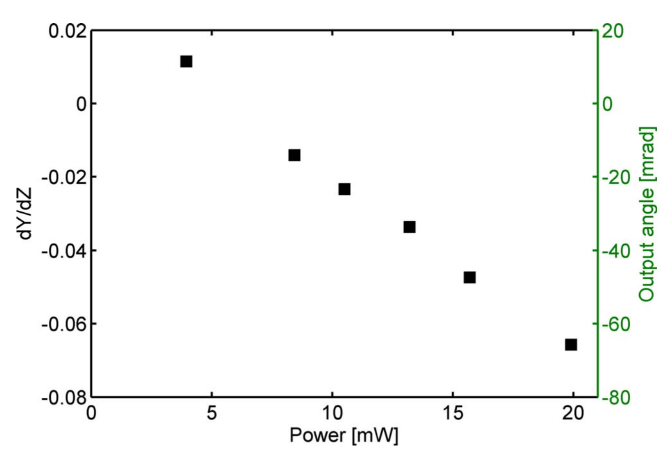

FIG. 5. (Color online) Output angle of nematicon as a function of input power.

[14], the nonlinear coupling due to $\theta^2 q_y$ in the momentum Eq. (8) causes a depression in the potential barrier as the nematicon amplitude (power) increases, allowing escape. These results and the method outlined here can be extended to explore guiding effects in a wide range of media with a refractive index change generated by other physical mechanisms, including thermal and photorefractive nonlinearities [7,22–24].

[1] G. B. Whitham, *Linear and Nonlinear Waves* (Wiley, New York, 1974).
[2] A. B. Aceves, J. V. Moloney, and A. C. Newell, Phys. Rev. A **39**, 1809 (1989).
[3] Y. Linzon, R. Morandotti, M. Volatier, V. Aimez, R. Ares, and S. Bar-Ad, Phys. Rev. Lett. **99**, 133901 (2007).
[4] P. Dumais, A. Villeneuve, A. Saher-Helmy, J. Stewart Aitchison, L. Friedrich, R. A. Fuerst, and G. I. Stegeman, Opt. Lett. **25**, 1282 (2000).
[5] A. B. Aceves, J. V. Moloney, and A. C. Newell, Phys. Rev. A **39**, 1828 (1989).
[6] B. Alfassi, C. Rotschild, O. Manela, M. Segev, and D. N. Christodoulides, Phys. Rev. Lett. **98**, 213901 (2007).
[7] A. Barak, O. Peleg, C. Stucchio, A. Soffer, and M. Segev, Phys. Rev. Lett. **100**, 153901 (2008).
[8] G. Assanto, M. Peccianti, and C. Conti, Opt. Photonics News **14**(3), 44 (2003).
[9] M. Peccianti and G. Assanto, Opt. Express **15**, 8021 (2007).
[10] M. Peccianti, A. Dyadyusha, M. Kaczmarek, and G. Assanto, Nat. Phys. **2**, 737 (2006).
[11] M. Peccianti, G. Assanto, A. Dyadyusha, and M. Kaczmarek, Phys. Rev. Lett. **98**, 113902 (2007).
[12] M. Peccianti, G. Assanto, A. Dyadyusha, and M. Kaczmarek, Opt. Lett. **32**, 271 (2007).
[13] A. Piccardi, G. Assanto, L. Lucchetti, and F. Simoni, Appl. Phys. Lett. **93**, 171104 (2008).
[14] M. Peccianti, A. Dyadyusha, M. Kaczmarek, and G. Assanto, Phys. Rev. Lett. **101**, 153902 (2008).
[15] A. A. Minzoni, N. F. Smyth, and A. L. Worthy, J. Opt. Soc. Am. B **24**, 1549 (2007).
[16] G. Assanto, N. F. Smyth, and A. L. Worthy, Phys. Rev. A **78**, 013832 (2008).
[17] I. C. Khoo, *Liquid Crystals: Physical Properties and Nonlinear Optical Phenomena* (Wiley, New York, 1995).
[18] G. Assanto and M. Peccianti, IEEE J. Quantum Electron. **39**, 13 (2003).
[19] C. Conti, M. Peccianti, and G. Assanto, Phys. Rev. Lett. **91**, 073901 (2003).
[20] D. J. Kaup and A. C. Newell, Proc. R. Soc. London, Ser. A **361**, 413 (1978).
[21] C. García-Reimbert, A. A. Minzoni, T. R. Marchant, N. F. Smyth, and A. L. Worthy, Physica D **237**, 1088 (2008).
[22] F. Derrien, J. F. Henninot, M. Warenghem, and G. Abbate, J. Opt. A, Pure Appl. Opt. **2**, 332 (2000).
[23] B. Crosignani, P. DiPorto, A. DeGasperis, M. Segev, and S. Trillo, J. Opt. Soc. Am. B **14**, 3078 (1997).
[24] W. Krolikowski, B. Luther-Davies, and Y. Kivshar, Opto-Electron. Rev. **9**, 287 (2001).